CHAPTER 5

Linear trinuclear complexes with aromatic bridges: Synthesis, Characterization, Redox Properties and Magnetic Exchange.

5.1 Introduction

5.2 Experimental

5.3 Results and Discussion

5.4 References

5.1 Introduction

Bifunctional aromatic bridging ligands occupy important position in the chemistry of multinuclear transition metal complexes. This is because they offer planar geometries in most cases and suitable π-symmetry orbitals, usually with complete π-delocalization over the bridging part of the ligand. These facilitate electron delocalization, spin exchange and hence, attribute interesting electrochemical and magnetic properties to the related complexes. The early examples of binuclear complexes with aromatic bridging groups involve the complexes with 2,5-dihydroxy benzoquinone,[1] 1,4-dihydroxy napthoquinone[2] and dihydroxy anthraquinone.[3] The complexes of these bridging ligands were found to be strongly exchange coupled, in spite of having large M····M distance. The complete planarity of these molecules and π-delocalization were obviously the attributed reasons for the strong spin exchange. Later, binuclear complexes of terephthalate[4] and the corresponding polynuclear chains[5] were observed to have moderately strong intramolecular antiferromagnetic exchange and strong intermolecular spin exchange.

A variety of nitrogen heterocycles and their derivatives[6-19] are known to be efficient mediators of spin exchange as described in Chapter 1. Among the diazine bridges,[20-27] it was found that pyridazine is more efficient mediator of spin exchange than phthalazine or dithiazole.[28] Binuclear copper complex with a binucleating Schiff base formed by the reaction of acetyl acetone with 1,2,4,5-tetraaminobenzene, where the metal ions are supported by a phenyl ring at a distance of 7.5Å, weak antiferromagnetic interaction with $J = -12\ cm^{-1}$ has been observed.[29] In the binuclear copper(II) complexes bridged by the ligand 2,5-dihydroxy-3,6-di-X-substituted-1,4-benzoquinone[30], where X = H, Cl, Br, I, NO_2, the singlet- triplet energy gap ranges from $-174.4\ cm^{-1}$ for $X = NO_2$ to $-25cm^{-1}$ for X = I. For the halo derivatives the magnitude of antiferromagnetic interaction varies as I>Br>Cl. Apparently, the magnitude of antiferromagnetic exchange increases with increase in the polarity or electron withdrawing character of X-substituted bridging ligands.[31] Copper complexes of hydroquinone containing Schiff bases have been reported as models for copper containing amine oxidases. These complexes derived from 2,5-dihydroxy benzaldehyde and 2,4,5-trihydroxy benzaldehyde, exist as phenoxo bridged dimers and undergo strong spin exchange. These complexes also form supramolecular assemblies through coordination and hydrogen bonding between the solvent molecules and metal centres or 2,5-dihydroxy part of the molecule.[32] A significant spin exchange interaction has been shown to exist through these phenoxo moieties. A ferromagnetically coupled bent trinuclear copper(II) complex was synthesized by incorporating μ-phenoxo, μ-syn-syn carboxylato and μ_3-chloro bridges. In 1975, the complexes of the Schiff bases of diacetyl resorcinol with diamines like, N,N-dialkylethylenediamine (a) and diethylenetriamine (b) were found to be having antiferromagnetically coupled metal centers.[33]

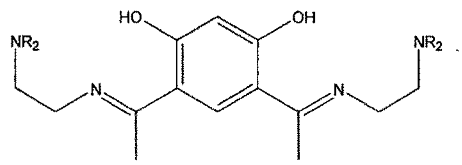

(a)

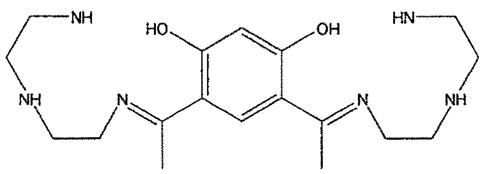

(b)

Macrocyclic dicopper(II) complexes derived from 2,6-di(R)formylphenols (c) and various linking diamines have been reviewed and their magnetic and structural properties have been discussed earlier.

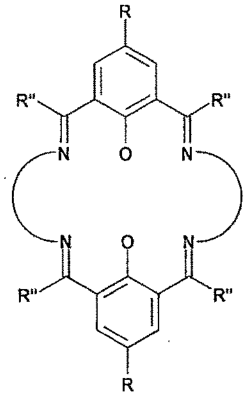

(c)

The functional groups present at 4-phenyl position (R) were varied from methyl, ethyl, t-butyl, $-CF_3$, the diamine part (R') was varied as $-(CH_2)_4-$, $-(CH_2)_3-$, $-(CH_2)_2-$, $-(CH_2CHOHCH_2)-$ and the group attached to the aromatic carbon (R'') as H or CH_3. All the complexes were found to have -2J values in the range 689-902cm^{-1}.[34]

Ferromagnetically coupled trinuclear copper(II) complex of a reduced Schiff base (d) was studied for its interaction with DNA. This complex forms a supramolecular structure through N-H$\cdots$Cl hydrogen bonding.[35]

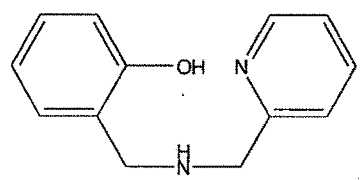

(d)

A series of trinuclear complexes involving two copper(II) ions with one uranium(IV), thorium(IV), or a zinc(II) with a series of Schiff base ligands, like (e), where, , are various aliphatic and aromatic diamines.

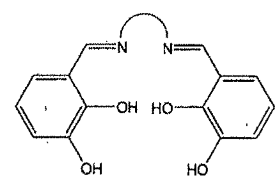

(e)

The geometrical parameters have a major influence on the magnetic properties of these complexes. For the smallest Cu$\cdots$U^{IV} distance, the Cu$\cdots$U^{IV} coupling is antiferromagnetic. It is weakly antiferromagnetic when the Cu$\cdots$U^{IV} distance is the largest. With thorium(IV) ion, the interaction is weak antiferromagnetic.[36]

Trimacrocyclic ligand 1,3,5-tris(1,4,7-triazacyclonon-1-ylmethyl)-benzene, (f)

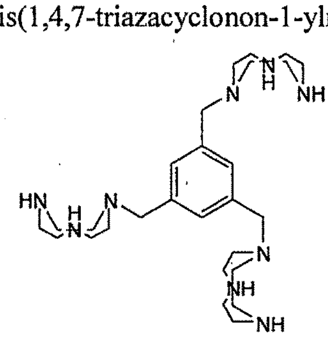

(f)

forms a hydroxo bridged trinuclear complex at natural pH. Above 9.5 pH it forms a hexanuclear copper complex, a dimer of trinuclear complex with S = ½, ground state, consistent with a system composed of an antiferromagnetically coupled copper(II) pair.[37] A mixed-valent $Cu^{I}Cu_2^{II}$ triangular metallomicrocycle was synthesized by reacting copper(II) salt and bis(N-salicyldene-4,4'-diphenylamine) (g),

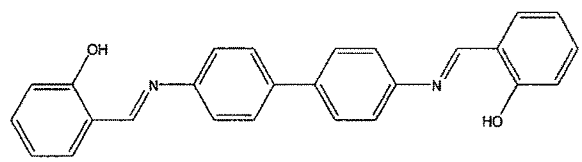

(g)

Magnetic study confirms the presence of two copper(II) ions and one copper(I) ion in a discrete triangular molecule. Strong intramolecular π-π interactions between the ligands are found to stabilize the constrained conformation of the triangle.[38] The first μ_3-oxalato-bridged copper(II) complex $[Cu_3(L)_3(\mu_3)C_2O_4]$ was reported with N-ethyl-N'-salicyldene-1,2-diaminoethane, (h).

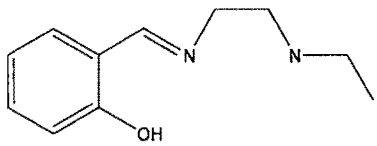

(h)

The tricopper unit was found to exhibit ferromagnetic coupling between the oxalate bridged copper atoms and antiferromagnetic coupling between the oxygen-bridged copper atoms.[39] Bi- and tripyridyl amine ligands (i, j, k and l) form trinickel and pentanickel complexes. These have increased solubility, stability and ability to form extended metal atom chains.[40] Similar chains with increased solubility and stability were synthesized with cobalt.[41]

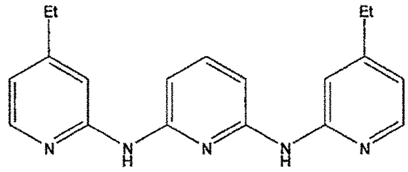

(i)

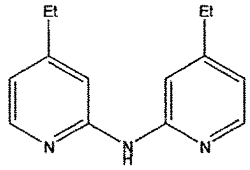

(j)

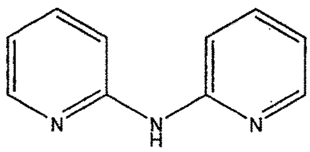

(k)

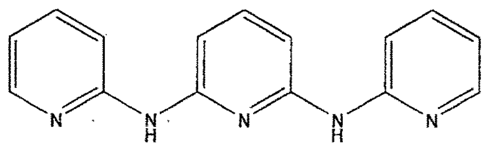

(l)

It has been observed that the ethyl substituents on the pyridyl ring in these complexes make them more soluble and allow them to carry oxidations easily. These complexes allow the complete examination of magnetic susceptibility as a function of temperature. N,N'-bis(2-hydroxyacetophenone)propylenediamine) (m),

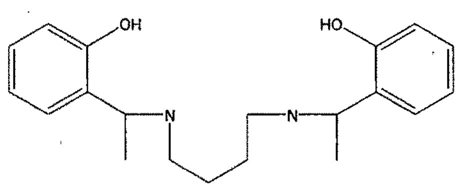

(m)

yielded two trinuclear Schiff base copper complexes. They were characterized by single crystal X-ray diffraction studies with a reasonable theoretical interpretation of the magnetic behavior shown by the complex.[42]

Most of the trinuclear complexes containing aromatic bridging moieties, reported so far are essentially discrete molecular assemblies, while very few are the complexes with specially designed trinucleating ligands. The later can have potential to offer specific coordination environment around the metal ions. Also modulation of structure and property becomes possible by adding various functional groups without much affecting the basic framework. Design of triangular complexes with such ligands is based on the biomolecule, enterobactin.

In order to see the efficacy of the trinucleating ligands with aromatic bridges in propagating magnetic exchange through their π-orbitals and to verify if the tuning of spin exchange is possible in such complexes by varying the nonbridging parts, three new trinucleating ligands have been synthesized by condensing 4,6-diacetyl resorcinol with three diamines namely, en, 2pn and 3pn. 4,6-diamino resorcinol provides a rigid back bone with aromatic bridging. A series of six new trinuclear copper(II) complexes has been synthesized using these ligands. The complexes have been characterized and their magnetic and electrochemical properties have been studied.

5.2. Experimental

Materials

AR quality en, 2pn and 3pn were purchased from Merck and were used without further purification. AR quality resorcinol (for the synthesis of 2,4-diacetyl resorcinol, **dar**) and sodium perchlorate (AR) were purchased from Merck. The chemicals and solvents used in the electrochemical studies were as described in Chapter 2. Solvents were used after distillation.

CAUTION: Perchlorate salts of metal complexes with organic ligands are potentially explosive. Only a small amount of material should be handled and with great caution.

Ligand Synthesis

Synthesis of dar: The ligand **dar** was synthesized by o-acylation of resorcinol following the Fries Rearrangement using a literature procedure.[23]

m. p. = 235°C.

Synthesis of the trinucleating **daren**

dar (0.2197g, 1.1324mmol) was dissolved in 10-15 ml of absolute ethanol, and the solution was allowed to reflux. 10-15 ml ethanolic solution containing **en** (0.034g, 0.0378ml, 0.5662mmol) was added slowly and drop wise through a dropping funnel to the refluxing solution. After half of the addition, yellow coloured crystalline solid started separating from the solution. After complete addition, the reaction mixture was stirred for 5 hrs under the reflux condition. The product was filtered, washed severally with ethanol and dried in air. The product was recrystallized from ethanol.

The other two ligands **dar2pn** and **dar3pn** were synthesized using the above procedure and using equivalent quantities of 1,2-diaminopropane (2pn) (For **dar2pn**) and 1,3-diaminopropane (3pn) (For **dar3pn**) in place of en.

The elemental analyses, physical constants and yields of all the three ligands are summarised in Table 5.1.

^{1}H NMR of daren: -CH_2 (4H, triplet, 3.6ppm), -CH_3 (12H, multiplet, 2.3ppm), Ar-H (2H, singlet, 6.1ppm), Ar-H, (2H, singlet, 7.8ppm), and Ar-O-H (2H, singlet, 12.43ppm) and Ar-O-H (2H, singlet, 17.01ppm). **(Fig.5.1)**

^{1}H NMR of dar2pn: -CH_3 (3H, doublet, 1.46ppm), -CH_3 (12H, multiplet, 2.5ppm), -CH_2 (2H, doublet, 3.8ppm), -CH (sextet, 1H, 4.32ppm), Ar-H (singlet, 2H, 6.31ppm), Ar-H (2H, doublet, 8.0ppm), Ar-O-H (2H, 12.69ppm) and Ar-O-H (2H, 17.23 ppm).

^{1}H NMR of dar3pn: -CH_3, (2H, quintet, 1.64ppm), -CH_3 (12H, multiplate 2.71ppm), -CH_2 (4H, triplet, 4.1ppm), Ar-H (2H, singlet, 6.54ppm), Ar-H (2H, singlet, 8.42ppm), Ar-O-H (2H, triplet, 12.8ppm) and Ar-O-H (2H, singlet, 17.48ppm).

Table 5.1 Yields, Analysis and physical constants of ligands.

Ligand	Yield (%)	Melting Point (^{0}C)	Elemental Analysis (%) C	H	N
daren	38.86	350 (dec.)	63.92	5.80	6.73
$C_{22}H_{24}O_6N_2$			(64.07)	(5.82)	(6.79)
dar2pn	37.28	240 (dec.)	64.73	5.85	6.50
$C_{23}H_{26}O_6N_2$			(64.78)	(6.10)	(6.59)
dar3pn	43.34	215 (dec.)	64.69	6.20	6.47
$C_{23}H_{26}O_6N_2$			(64.78)	(6.10)	(6.59)

Scheme 5.1 Scheme of ligand and complex synthesis

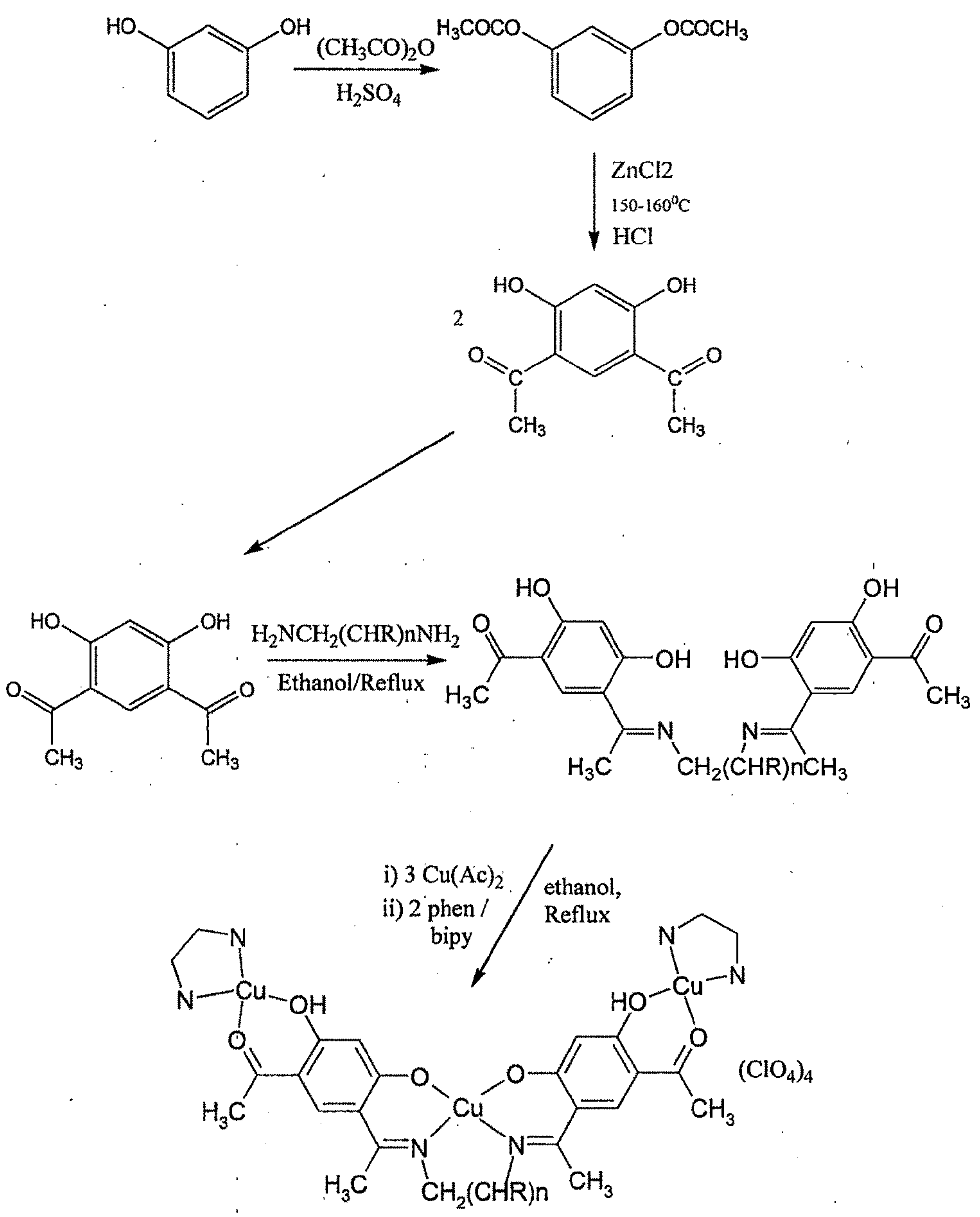

Where, daren, R = H, n = 1,

dar2pn, R = CH_3, n = 1 and

dar3pn, R = H, n = 2

is phen or bipy.

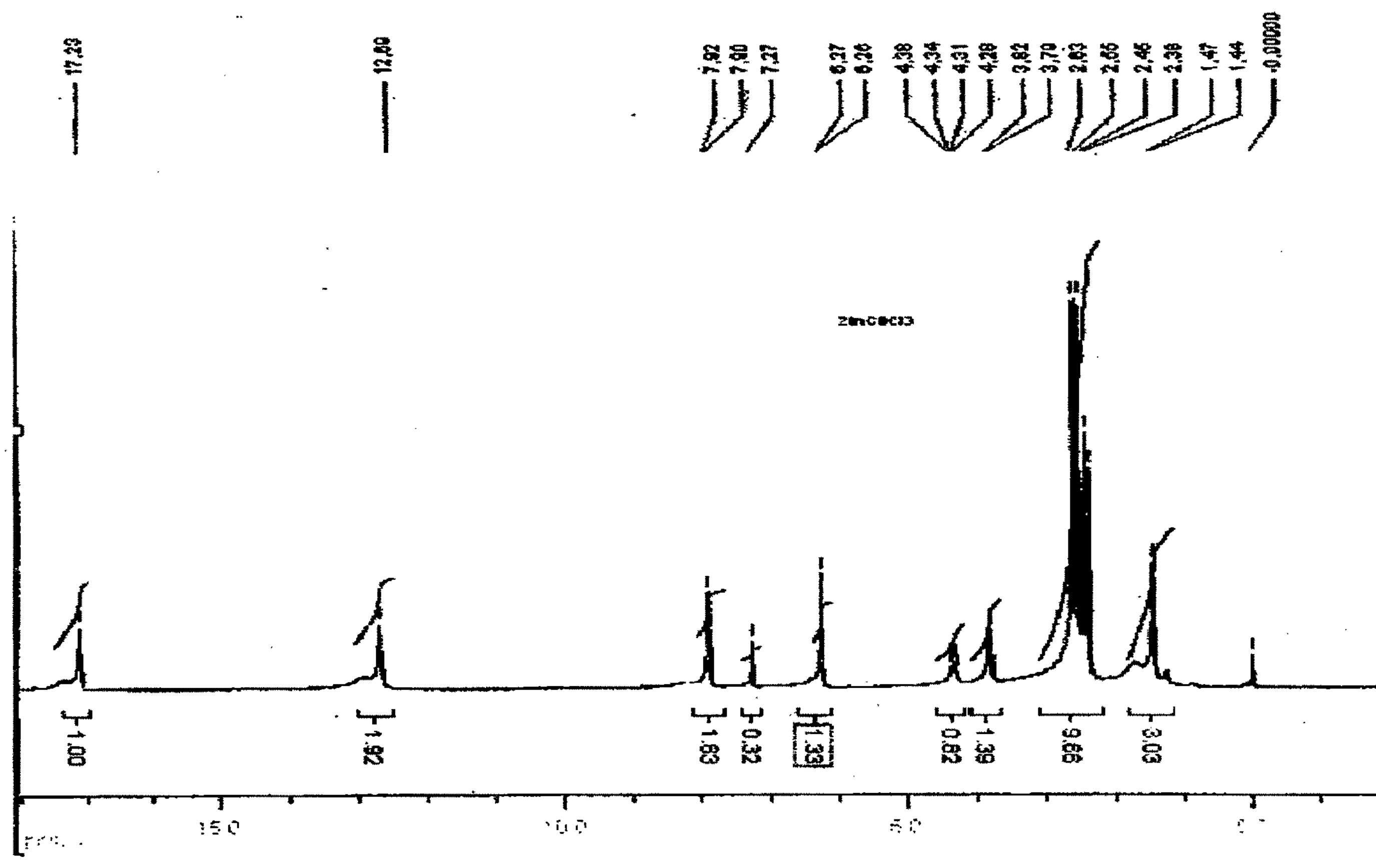

Fig.5.1 ^{1}H NMR of the ligand **daren**.

Synthesis of Complexes

i) **Synthesis of [Cu_3daren(phen)$_2$](ClO_4)$_4$ (5.1)**

0.206g (0.5mmoles) of ligand **daren** was taken in 10ml of ethanol and 0.206g (1.04mmoles, 4% excess) phen was added in the same solution in 100ml flask. This suspension was heated to reflux, where upon phen was dissolved completely but **daren** remained partly dissolved. In hot condition, 25ml ethanolic solution containing 0.311g (1.56mmoles, 4% excess) copper acetate monohydrate was added slowly and drop wise through a dropping funnel. As the addition of copper acetate started the light yellow colored solution first turned to light green and gradually became dark green as the addition continued. All contents of the reaction mixture dissolved and small amount of brown coloured solid separated. The solution along with the solid was then allowed to reflux for 5hrs. It was cooled to room temperature, the brown solid was filtered and washed with ethanol. All washings were collected. In the filtrate, aqueous-ethanol solution of sodium perchlorate was added with constant stirring till the precipitation of complex appeared to be complete. A dark green colored microcrystalline solid separated out. It was filtered, washed with ethanol (5 × 6ml) and dried in air at ~ 60-70^{0}C.

Other five complexes, with [Cu_3daren(bipy)$_2$](ClO_4)$_4$ **(5.2),** [Cu_3dar2pn(phen)$_2$](ClO_4)$_4$ **(5.3),** [Cu_3dar2pn(bipyp)$_2$](ClO_4)$_4$ **(5.4),** [Cu_3dar3pn(phen)$_2$](ClO_4)$_4$ **(5.5)** and [Cu_3dar3pn(bipy)$_2$](ClO_4)$_4$ **(5.6)** have been synthesized by following the same procedure as above and taking appropriate equivalent quantities of dar2pn or dar3pn in place of daren and either bipy or phen as bidentate capping ligand.

Physical Measurements

All the physical measurements, cyclic voltammetric studies, FAB-Mass analysis and ESR spectra were recorded using the instruments as mentioned earlier in chapter 2. (page no.79)

5.3. Results and Discussion

Characterization of the ligands

All the three trinucleating ligands, synthesized by above methods have been characterized by elemental analysis, FTIR and ^{1}H NMR spectroscopic techniques. The elemental analysis was found to be matching with the proposed formulae. In the FTIR spectra of the ligands (**Fig.5.6 to 5.8**) $\nu_{>C=O}$ has been observed between 1620-1640cm^{-1} while the $\nu_{>C=N-}$ is observed at ~1600cm^{-1}. The δ_{OH} and ν_{C-O} corresponding to the phenolic groups are observed at ~1250-1280 and 1320-1380cm^{-1}, respectively. Besides these, the ν_{C-C} (aromatic), δ_{C-H} (aromatic) and δ_{C-H} (-CH_2) are observed, respectively, between 1450-1580, ~830 and between 1440-1490cm^{-1} regions. The presence of these bands in the IR spectra of the ligands supports their formation.

Characterization of the trinuclear complexes of dar derivatives.

The elemental analyses of the complexes agree with the values calculated from the suggested formulae as can be seen in Table 5.2.

Table 5.2 Yield and elemental analysis of the complexes.

Complex	Yield %	Elemental Analysis (%)			Molar Cond. $\Omega^{-1}cm^{-1}mol^{-1}$
		C	H	N	
[Cu_3daren(phen)$_2$](ClO_4)$_4$ $C_{46}H_{36}O_{22}N_6Cu_3Cl_4$	35.15	40.22 (40.68)	2.52 (2.65)	6.49 (6.19)	240
[Cu_3daren(bipy)$_2$](ClO_4)$_4$ $C_{42}H_{36}O_{22}N_6Cu_3Cl_4$	28.62	38.21 (38.51)	2.75 (2.75)	6.90 (6.41)	240
[Cu_3dar2pn(phen)$_2$](ClO_4)$_4$ $C_{47}H_{40}O_{22}N_6Cu_3Cl_4$	32.32	42.55 (42.08)	2.72 (2.91)	6.75 (6.11)	220
[Cu_3dar2pn(bipy)$_2$](ClO_4)$_4$ $C_{43}H_{40}O_{22}N_6Cu_3Cl_4$	40.29	39.21 (39.01)	2.67 (2.87)	6.31 (6.37)	59
[Cu_3dar3pn(phen)$_2$] (ClO_4)$_4$ $C_{47}H_{40}O_{22}N_6Cu_3Cl_4$	36.05	43.95 (44.20)	3.11 (3.08)	6.45 (6.31)	180
[Cu_3dar3pn(bipy)$_2$] (ClO_4)$_4$ $C_{43}H_{40}O_{22}N_6Cu_3Cl_4$	16.26	38.93 (38.48)	2.89 (2.98)	6.24 (6.26)	220

Molar conductivity of the six complexes in 1.0mM solutions in DMF ranges between 180-240 $\Omega^{-1}cm^{-1}mol^{-1}$ except **[Cu$_3$dar2pn(bipy)$_2$](ClO$_4$)$_4$**, where it is observed to be much lower.

The molar conductivity values suggest that the perchlorate anions are not coordinated with the metal ions and are present outside the coordination sphere. Lower conductivity, value in the complex containing bipy indicates weak perchlorate coordination in this complex.

FAB Mass

Two representative complexes **[Cu$_3$daren(phen)$_2$](ClO$_4$)$_4$** and **[Cu$_3$dar2pn(bipy)$_2$]-(ClO$_4$)$_4$** were analyzed by FAB-Mass spectrometry (**Fig.5.2 & 5.4**). The complexes have perchlorate anions and hence can get readily disintegrated under FAB conditions. Also, they can hold more number of protons. It has been observed that the complex **[Cu$_3$daren(phen)$_2$](ClO$_4$)$_4$**, readily loses one phen and perchlorates to form the most abundant species. These and other important species listed in the Table 5.3 confirm the formation of the molecule with suggested formulae. A number of high molecular weight species formed by association of the fragments and copper clusters have also been identified.

Table 5.3 FAB-Mass of Complex **[Cu$_3$daren(phen)$_2$](ClO$_4$)$_4$.**

Sr. No.	Fragments	m/Z (Cal.)	m/Z (obs.)
1.	[Cu$_3$daren(phen)$_2$]2H$_2$O$^+$	994	994
2.	[Cu$_3$daren(phen)$_2$]2H$_2$O^{2+}/2	498	498
3.	[Cu$_3$daren(phen)]H$_2$O$^+$	796.62	796
4.	[Cu(Phen)$_2$]$^+$	423	423
5.	[Cuphen]$^+$	243	243
6.	[Cudaren]$^+$	470	470
7.	[daren]$^+$	412	412
8.	[Cudaren(Phen)]H$_2$O^{2+}/2	396	396
9.	[Cu$_3$daren(phen)$_2$]$^{4+}$/4	239.5	240

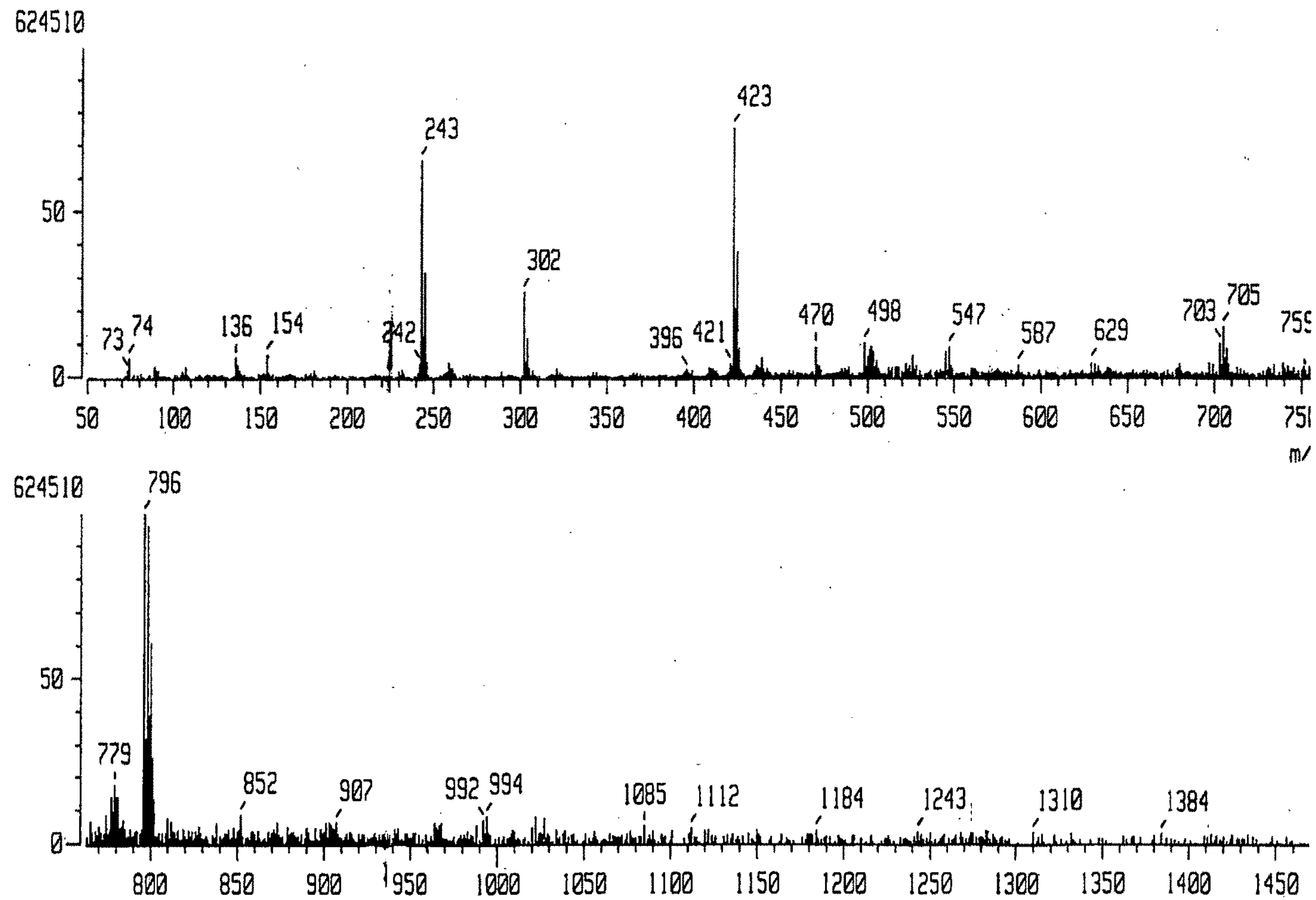

Fig.5.2 FAB-Mass spectrum of complex **[Cu_3daren(phen)$_2$](ClO_4)$_4$**

The important fragments are drawn below.

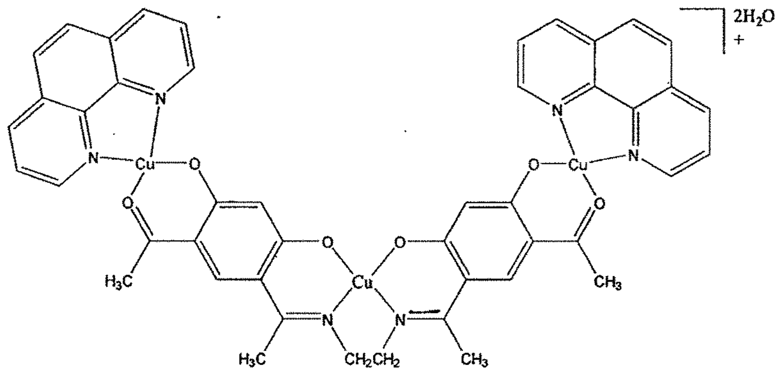

observed at m/Z at 994.

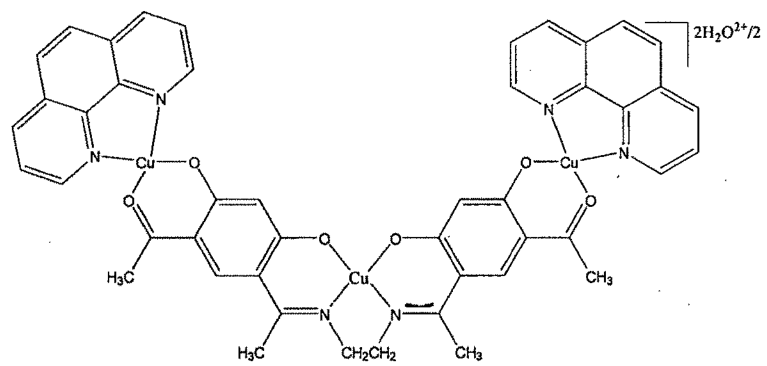

observed at m/Z 498 (498).

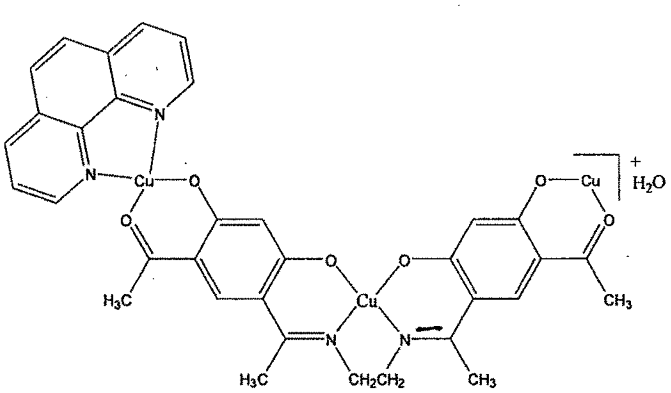

observed at m/Z at 797 (796).

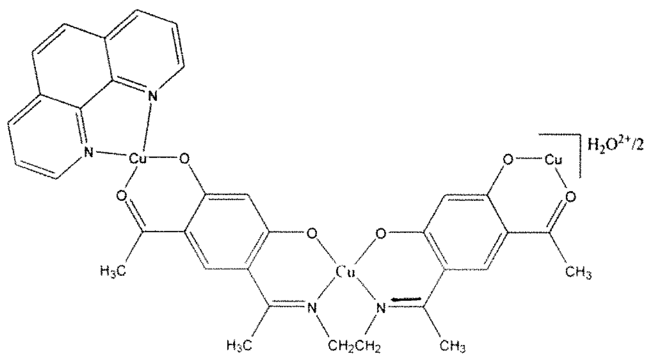

Observed at m/Z = 396.

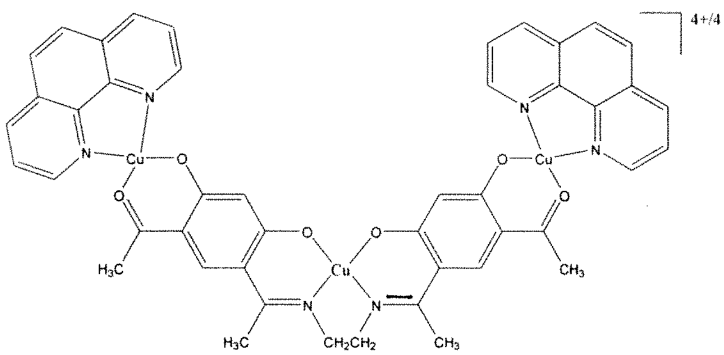

observed at m/Z at 240 (240).

Fig.5.3

Table 5.4 FAB-Mass of Complex **[Cu_3dar2pn(bipy)$_2$](ClO_4)$_4$**.

Sr. No.	Fragments	m/Z (Cal.)	m/Z (obs.)
1.	[Cu_3dar2pn(bipy)$_2$](ClO_4)$_4$+4H^+/4	332	332
2.	[Cu_3dar2pn(bipy)$_2$]$^{4+}$/4	231	231
3.	[Cu_3dar2pn(bipy)$_2$](ClO_4)$_4$+H^+/2	609	609
4.	[Cu_3dar2pn(bipy)$_2$](ClO_4)$_2$+2H^+/4	280	280
5.	[Cu_3dar2pn(bipy)$_2$]ClO_4^{3+}+H^+/4	254	254
6.	[Cu_3dar2pn(bipy)$_2$]ClO_4^{2+}/2	511	511
7.	[Cu_2dar2pnbipy]$^+$	705	705
8.	[dar2pn]+H^+	427	427
9.	[Cudar2pn]+H^+	488	488
10.	[Cubipy]+H^+	219	219
11.	[Cu(bipy)$_2$]+H^+	375	375

Because of the presence of readily ionisable perchlorate the parent cations are readily formed. The peak corresponding to the protonated complex has been observed at m/z = 332. The tetra cationic complex without any perchlorate has high abundance with m/z = 232. Peaks indicating sequential loss of perchlorate anions are observed at m/z = 332, 609, 280 and 254 respectively. Some other important fragments are also identified and are listed in Table 5.4. Thus the formation of the trinuclear complex with the suggested formula can be confirmed.

FAB-Mass analysis and the fragments observed and reported above support the formation of the complexes as per the given structural formula.

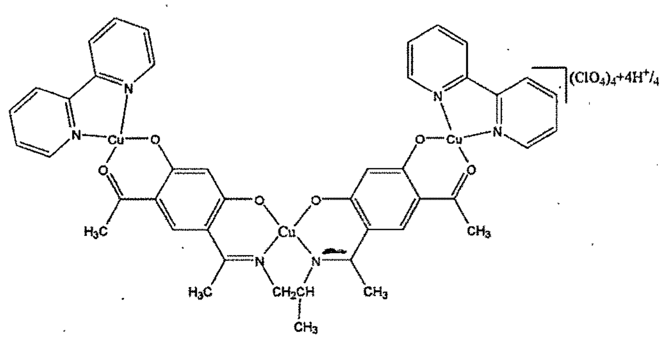

observed at m/Z at 332 (332).

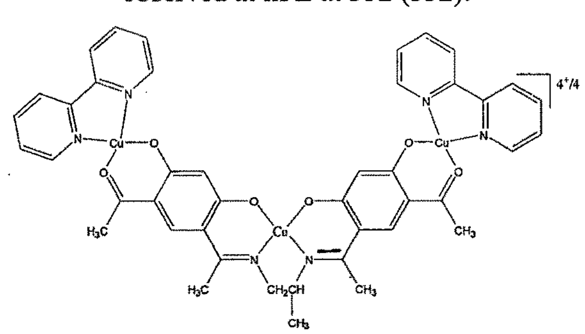

observed m/Z at 232 (231.15)

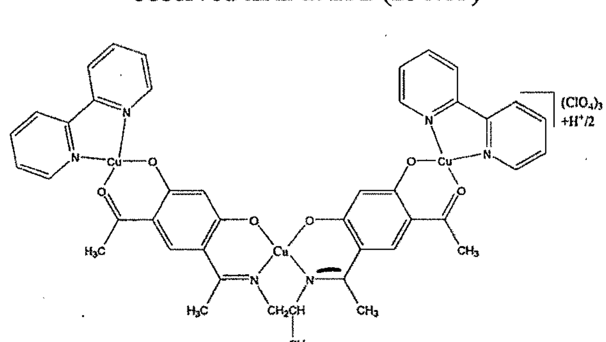

observed m/Z at 609 (609).

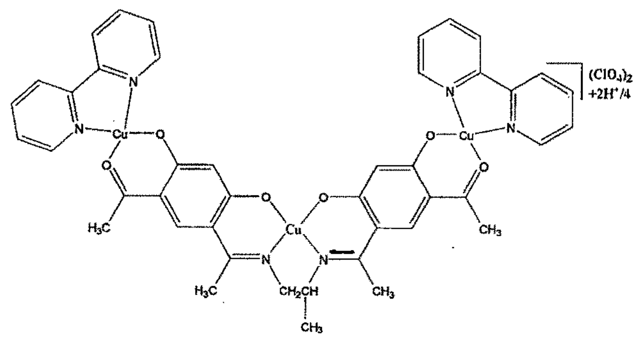

observed m/Z at 280 (280).

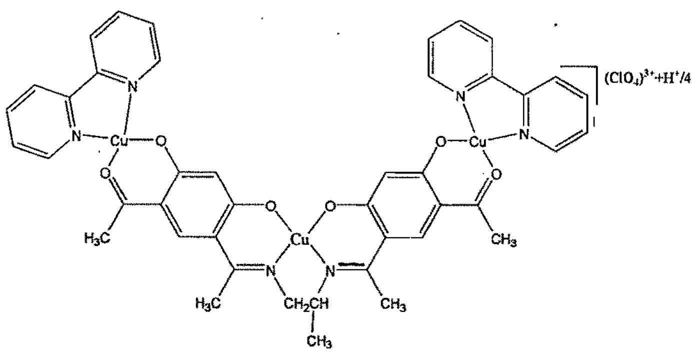

observed at m/Z at 255 (255).

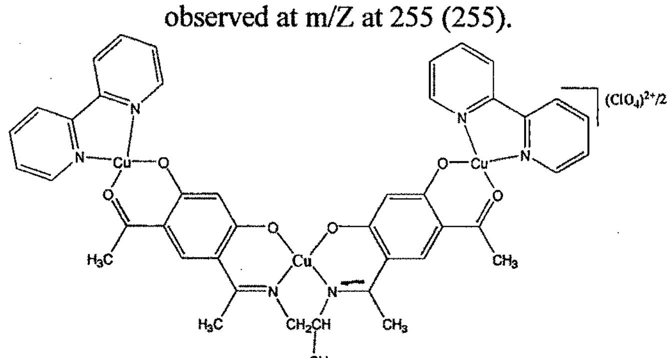

observed at m/Z = 511 (512)

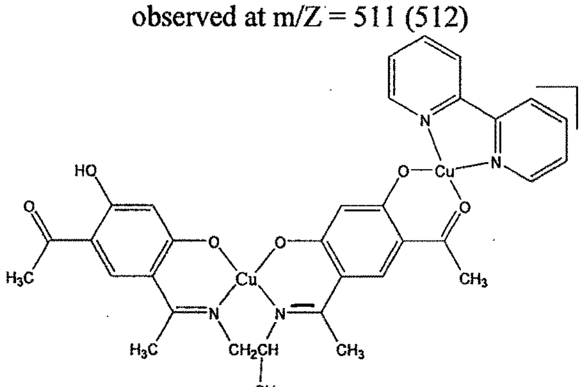

observed at m/Z 705 (706).

Fig.5.4

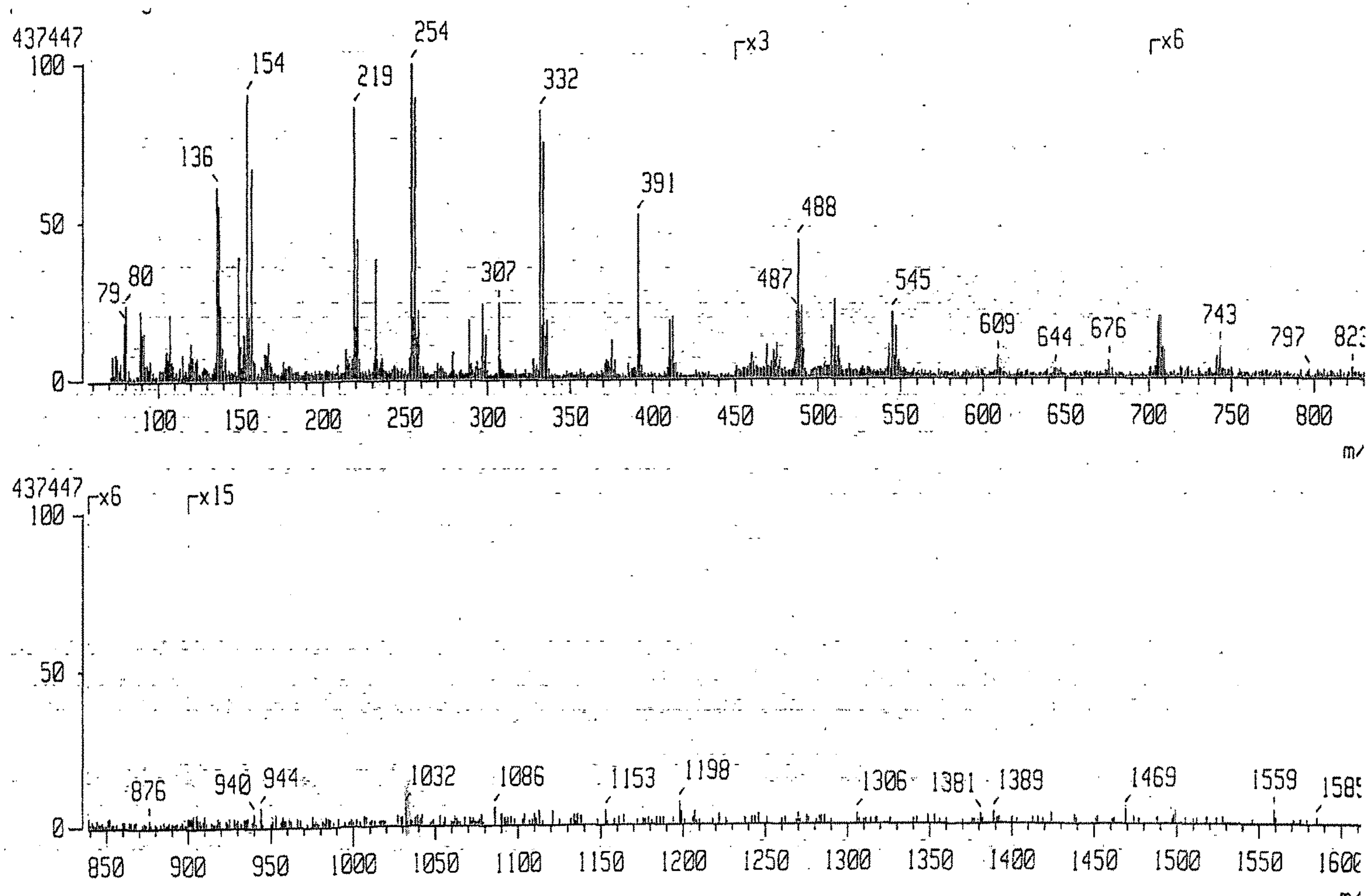

Fig. 5.5 FAB-Mass spectrum of complex **[Cu_3dar2pn(bipy)$_2$](ClO_4)$_4$**.

Electronic and Vibrational Spectra

Table 5.5 Electronic spectral analysis.

Complex	λ_{max} (400-900nm)	λ_{max} (200-400nm)
$[Cu_3daren(phen)_2](ClO_4)_4$	585	205,272,294.
$[Cu_3daren(bipy)_2](ClO_4)_4$	607	206,299,310.
$[Cu_3dar2pn(phen)_2](ClO_4)_4$	633	206,272,294.
$[Cu_3dar2pn(bipy)_2](ClO_4)_4$	711	205,300.
$[Cu_3dar3pn(phen)_2](ClO_4)_4$	625	205,272,294,364.
$[Cu_3dar3pn(bipy)_2](ClO_4)_4$	637	206,247,299.

The electronic spectra of the complexes in methanolic solutions exhibit intraligand transitions in 205-310nm region. The characteristic π- π^* transition in phen is observed at 272nm in complex **$[Cu_3daren(phen)_2](ClO_4)_4$**, **$[Cu_3dar2pn(phen)_2](ClO_4)_4$** and **$[Cu_3dar3pn(phen)_2](ClO_4)_4$**. The π- π^* transition characteristic of bipy is observed at 310, 300 and at 299nm in the complexes **$[Cu_3daren(bipy)_2](ClO_4)_4$**, **$[Cu_3dar2pn(bipy)_2](ClO_4)_4$** and **$[Cu_3dar3pn(bipy)_2](ClO_4)_4$**. n- π^* transitions in phen and bipy at around 323 and 235nm are absent. Weak and broad bands corresponding to the ligand field transitions in copper(II) are observed between 585-715nm. The absorption at longer wavelengths in spite of the presence of strongly coordinating bipy or phen indicates that the geometry of the complexes must be distorted from regular square planar geometry.

The FTIR spectra of the complexes (**Fig.5.6 to 5.8**) include all main features of the trinucleating ligands, the capping ligands and the perchlorate anion. The carbonyl stretching frequency ($\nu_{>C=O}$) in the complexes has been observed between 1584-1602cm^{-1}. These are shifted to lower energy as compared to their parent ligands by approximate 20-60cm^{-1}. A similar shift towards lower frequencies is observed in the imine stretching ($\nu_{>C=N}$) in all the complexes. The shift in both of these vibrations confirms the involvement of these groups in coordination with the metal ion. The bands corresponding to the δ_{O-H} and ν_{C-O} in the phenolic part of the ligands also have been observed to be shifted towards lower frequencies by ~5-10cm^{-1}. Thus it is evident that the phenolate –O-H (at least one) remains protonated in the complexes. The C-C multiple bond stretchings (in the aromatic rings) have been observed at 1534-1538cm^{-1} in the ligands. These are found to appear at 1518-1520cm^{-1} in the complexes of phen and at 1492-1496 in the complexes containing bipy. The presence of characteristic features of perchlorate anion at 626 and 1088-1090cm^{-1} in all complexes confirms their presence and also the ionic nature of perchlorate in the complexes. The important bands observed in the IR spectra of the ligands and the complexes are summarized in Table - 5.7.

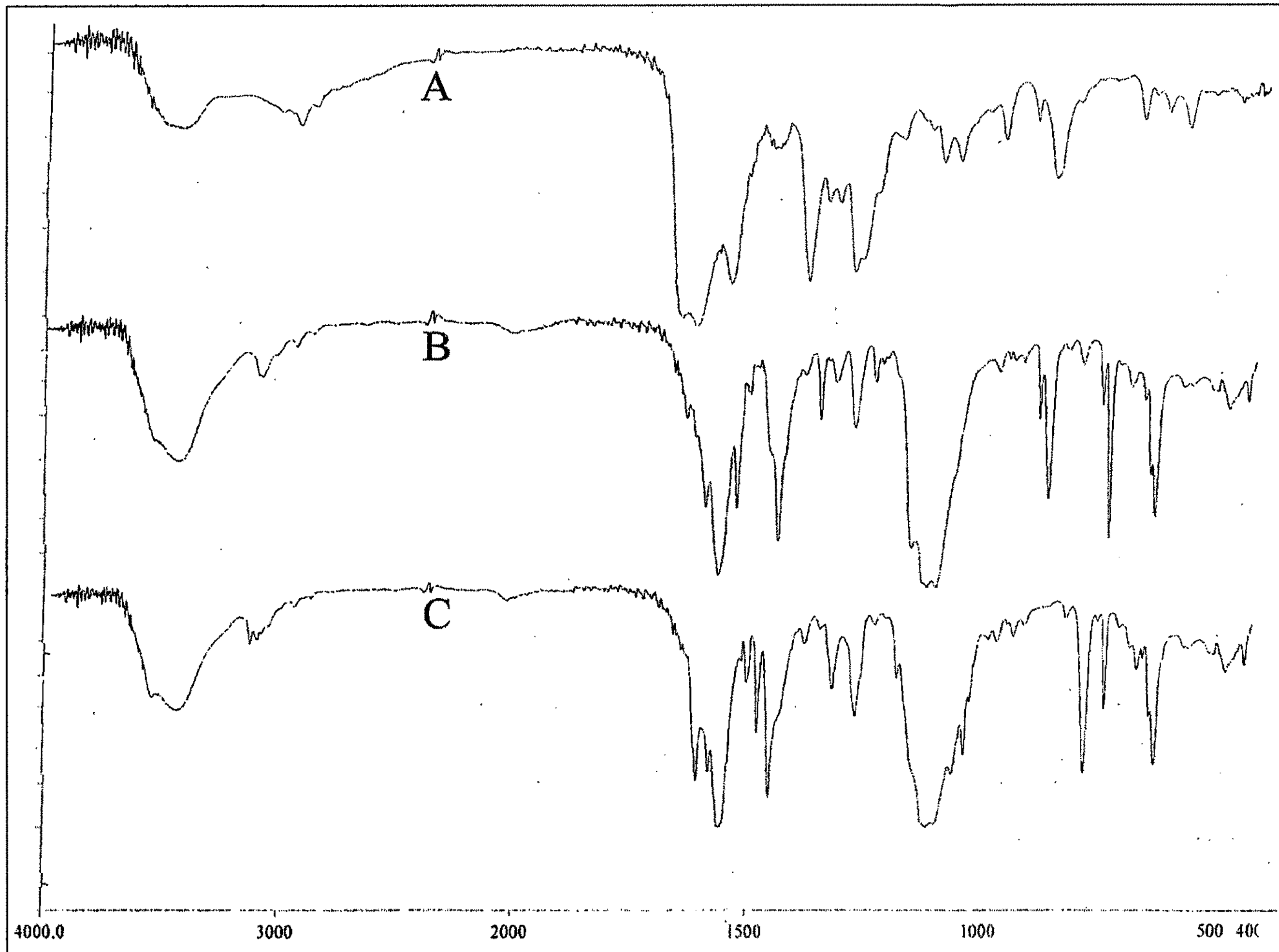

Fig. 5.6 FTIR spectra of ligand **daren (A),** and complexes **$[Cu_3daren(phen)_2](ClO_4)_4$ (B)** and **$[Cu_3daren(bipy)_2](ClO_4)_4$ (C).**

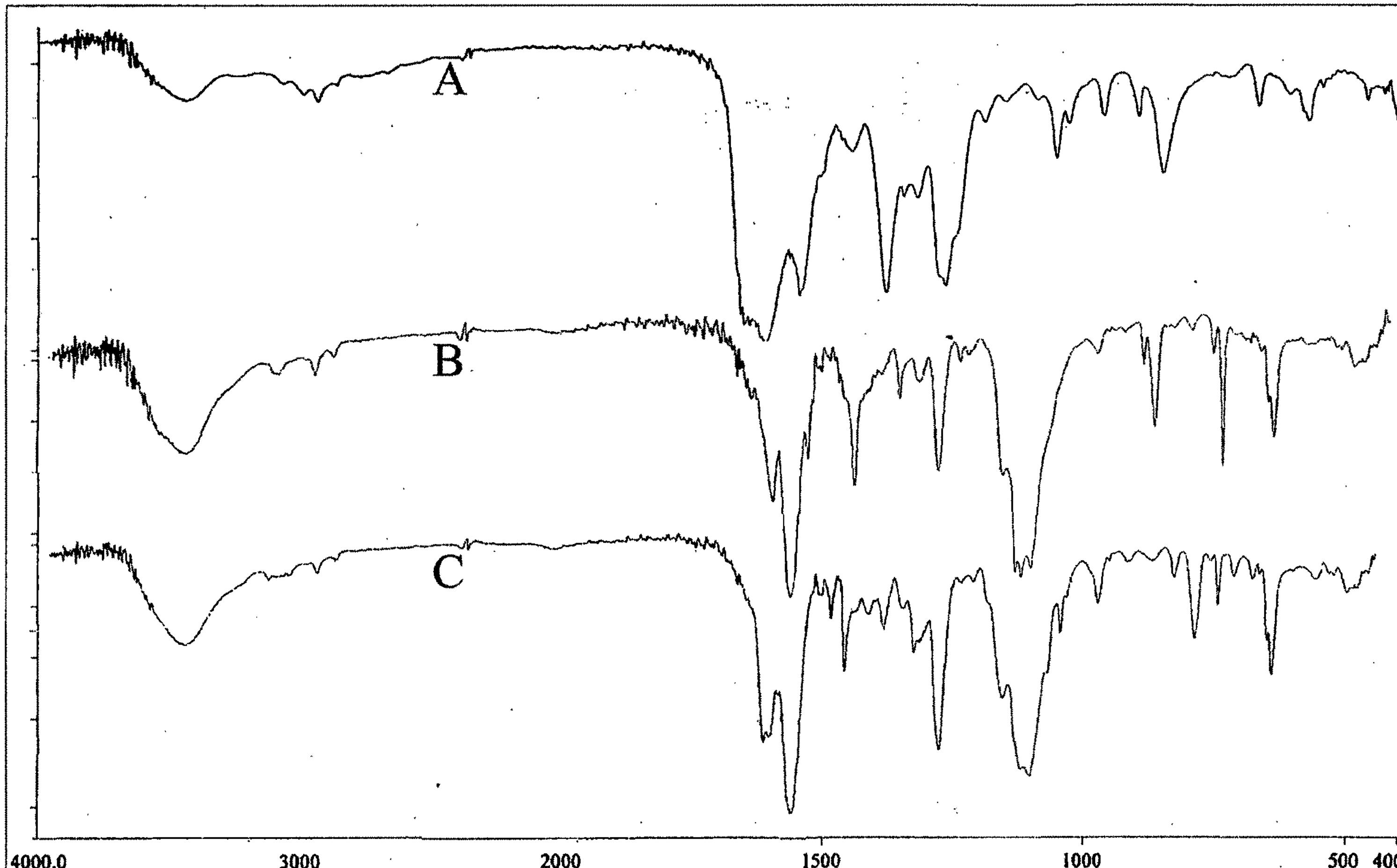

Fig. 5.7 FTIR spectra of ligand **dar2pn (A)** and complexes **[Cu_3dar2pn(phen)$_2$](ClO_4)$_4$ (B)** and **[Cu_3dar2pn(bipy)$_2$](ClO_4)$_4$ (C).**

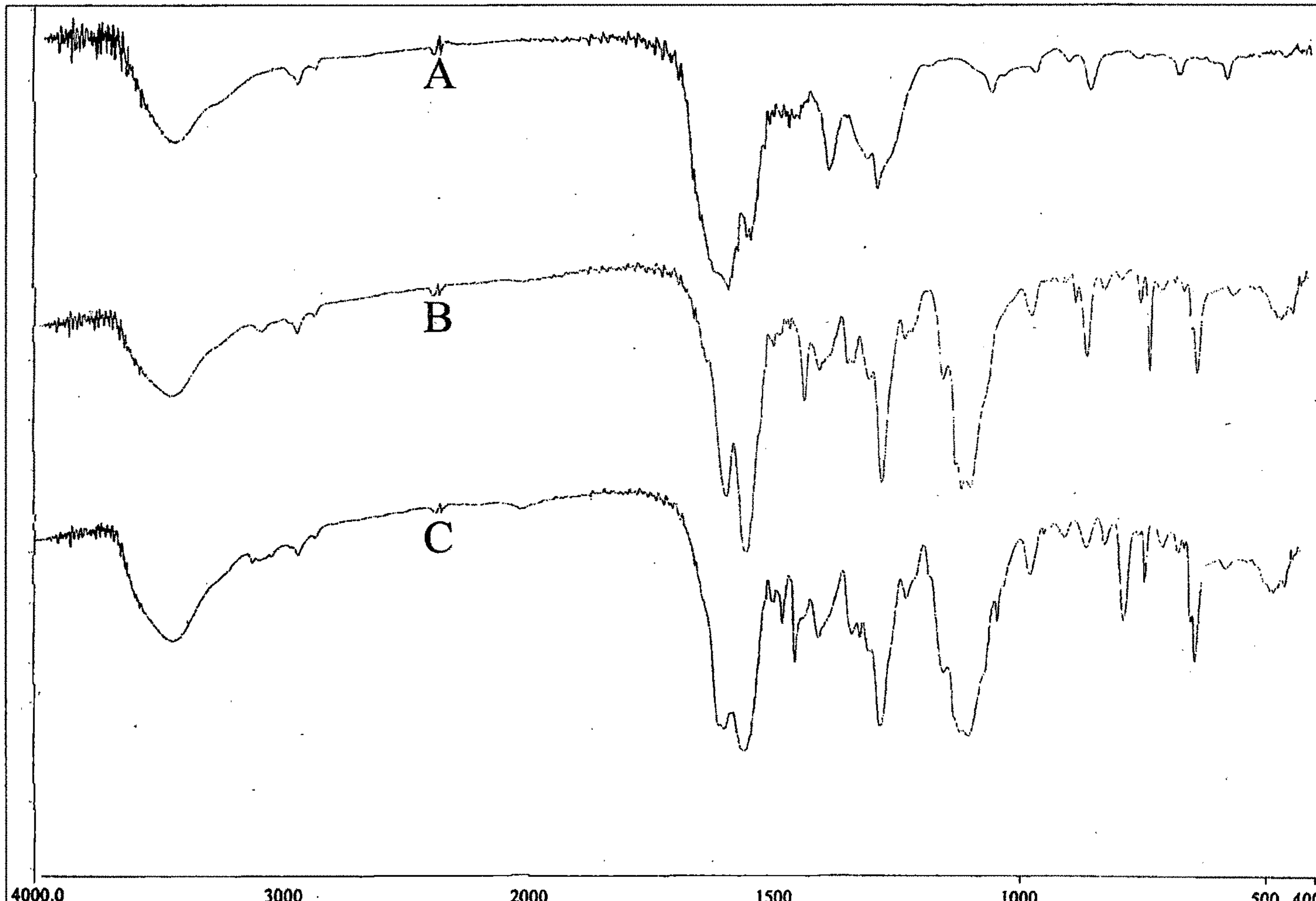

Fig. 5.8 FTIR spectra of ligand **dar3pn, (A)** and complexes **[Cu_3dar3pn(phen)$_2$](ClO_4)$_4$ (B)** and **[Cu_3dar3pn(bipy)$_2$](ClO_4)$_4$ (C).**

Table 5.6 FTIR spectral data of Ligands and Complexes.

Freq.	Ligands			Complexes					
	daren	**dar2pn**	**dar3pn**	**5.1**	**5.2**	**5.3**	**5.4**	**5.5**	**5.6**
>C=N-	1633.	1640.	1624.	1584.	1602.	1585.	1602.	1587.	1590.
>C=O	1605.	1605.	1578.	1556.	1553.	1552.	1547.	1547.	1549.
Alp.>C-N-	1051, 1087.	1048, 1090, 1195.	1047.	961, 909.	928, 962, 1032.	1150.	1143, 1120.	964.	1033.
-O-H (b) & -C-O (s) in Phenols	1270 &1329, 1368.	1258 &1320, 1371.	1276, 1375.	1267,1308, 1348.	1263, 1313, 1380.	1267, 1341.	1264,1314, 1372.	1276,1340, 1398.	1270, 1314, 1330.
-C-C - multiple bond strech (Arm.)	1534.	1538.	1534.	1518.	1496.	1518.	1492.	1520.	1492.
Phen.	------	------	------	636,722, 781,852, 1109.	------	722,852, 873,1108.	------	722,776, 850,874, 1108.	------
Bipy.	------	------	------	------	625,731, 774,928, 962,1110.	------	626,730, 774,961, 1106.	------	625,731, 773,967, 1107.
-O-H	3438	3434	3422	3422	3422	3422	3434	3448	3431
$-ClO_4$	------	------	------	627, 1088.	625, 1088.	626, 1088.	626, 1090.	624, 1088.	626, 1090.

5.4 Molecular modelling

The geometry of the ligands has been optimized by *ab initio* quantum mechanical calculations[43-54] using 6-31G basis set. It has been observed that the phenolate –C-O, imine C-C (ring) and carbonyl C-C (ring) bond distances increase with a small decrease in the carbonyl >C=O and imine >C=N bond distances. This suggests the presence of delocalization of π–electron density from carbonyl oxygen to phenolate oxygen and to the imine N through the phenyl ring. Thus, the part of the trinucleating ligand bridging between the terminal and the central copper(II) ions has complete π delocalization with more or less planar geometry and hence should behave as an efficient mediator for delocalisation of metal electron density/ spin density over the neighbouring metal ions. Thus, a strong magnetic exchange and antiferromagnetism may be expected. The plots of ESP over electron density show large amount of electron density over the phenolic oxygen, carbonyl oxygen and imine nitrogens thus confirming that these are the preferred coordinating sites in these ligands.

The trinuclear complex molecules contain more than 100 molecules and 3 heavy atoms. Such systems are very difficult for geometry optimization by *ab intio* quantum mechanical calculations. Hence, the geometry of the complexes has been calculated using universal force field[43-54]. They are shown in **Fig.5.12** to **5.17**. The dihedral angles between the metal coordination planes have also been calculated and presented in Table 5.8. An attempt is made to correlate these values with the coupling constants.

This electron density distribution supports the N_2O_2 coordination of the ligands to the metal centers. These complexes were found to be antiferromagnetic in nature. This antiferromagnetism was also supported by the dihedral angles calculated from the optimized geometries of the complexes by semi empirical quantum mechanical calculations using Universal Force Field (UFF) method. The presence of two aromatic rings in ligands and the resonance of imine nitrogen help the central copper(II) ion to delocalize the electron density all over the complex. Electron densities are calculated and are found to be maximum at the coordinating atoms as can be seen in **Fig.5.10**.

Table 5.7 Bond distances in the ligands.

Ligands	Ar-C···O-H	C=O
daren (Fig.5.9)	1.349, 1.372, 1.368, 1.352	1.234 & 1.236
dar3pn (Fig.5.11)	1.350, 1.277, 1.353, 1.350	1.237 & 1.236

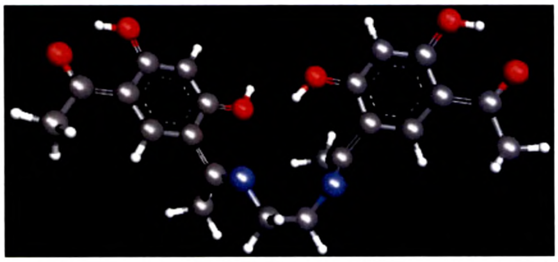

Fig.5.9 Optimized geometry of the ligand **daren** using 6-31G basis set.

As we see the plot between the electron density and electrostatic potentials for the ligands **daren** and **dar2pn**, the maximum electron density was found to be localized on, all the six oxygen and the two imines nitrogen (red color).

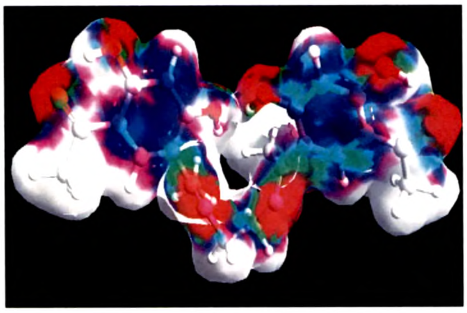

Fig.5.10 Plot of electrostatic potential over electron density in the ligand **daren**.

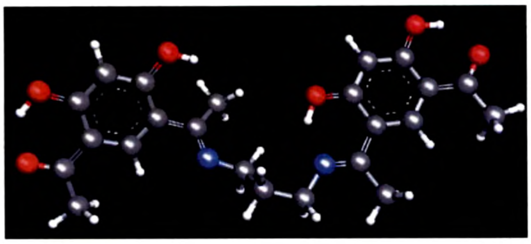

Fig.5.11 Optimized geometry of the ligand **dar3pn**. (6-31G basis set).

The geometry of the six trinuclear complexes have been optimized by semiemperical quantum mechanical calculation by Universal Force Field (UFF). The dihedral angles between the coordination planes have been calculated and compared with the extent of magnetic exchange.

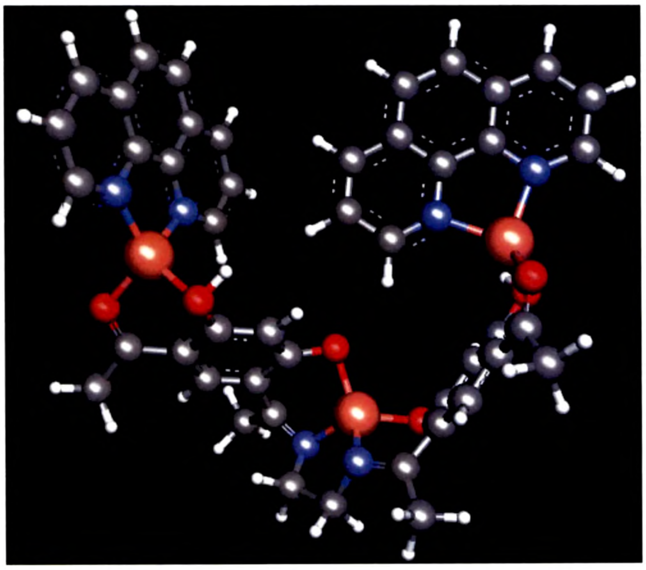

Fig.5.12 Optimized geometry of the complex **[Cu_3daren(phen)$_2$](ClO_4)$_4$** optimized using UFF.

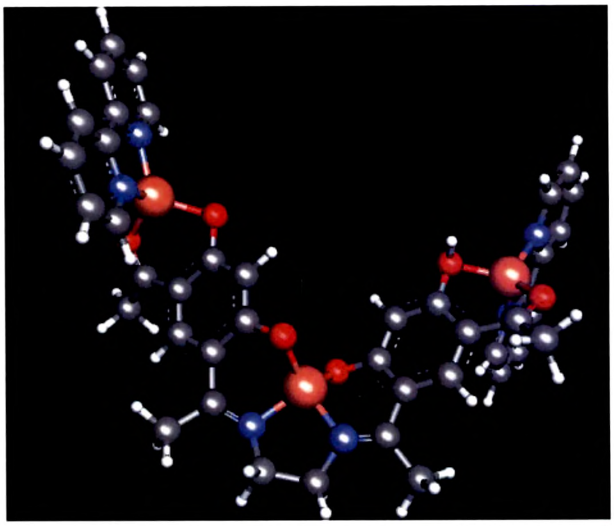

Fig.5.13 Geometry of the complex **[Cu_3daren(bipy)$_2$](ClO_4)$_4$** optimized using UFF.

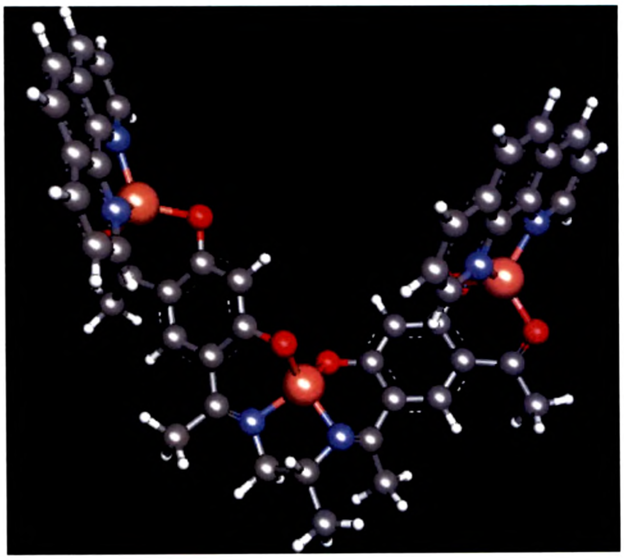

Fig.5.14 Optimized geometry of the complex **[Cu_3dar2pn(phen)$_2$](ClO_4)$_4$** optimized using UFF.

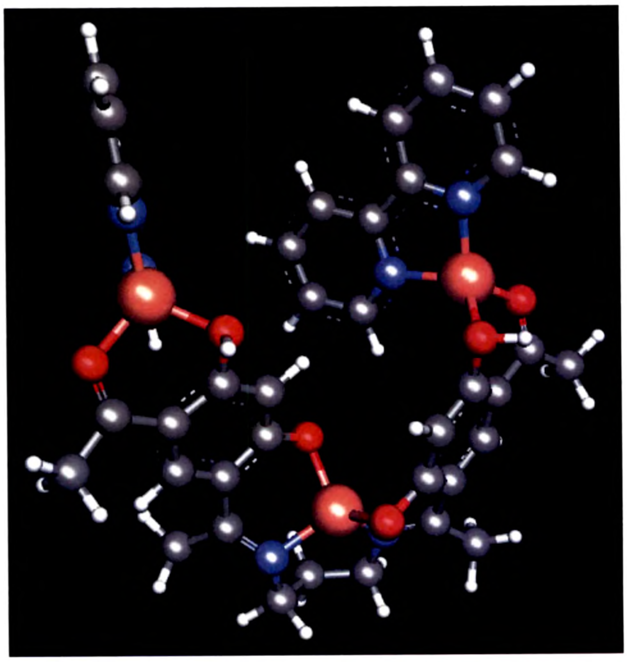

Fig.5.15 Optimized geometry of the complex **[Cu_3dar2pn(bipy)$_2$](ClO_4)$_4$** optimized using UFF.

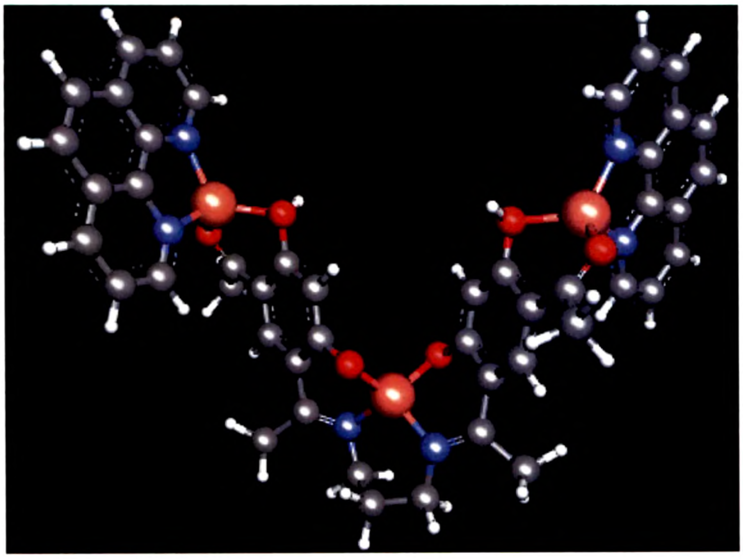

Fig.5.16 Optimized geometry of the complex **[Cu_3dar3pn(phen)$_2$](ClO_4)$_4$** optimized using UFF.

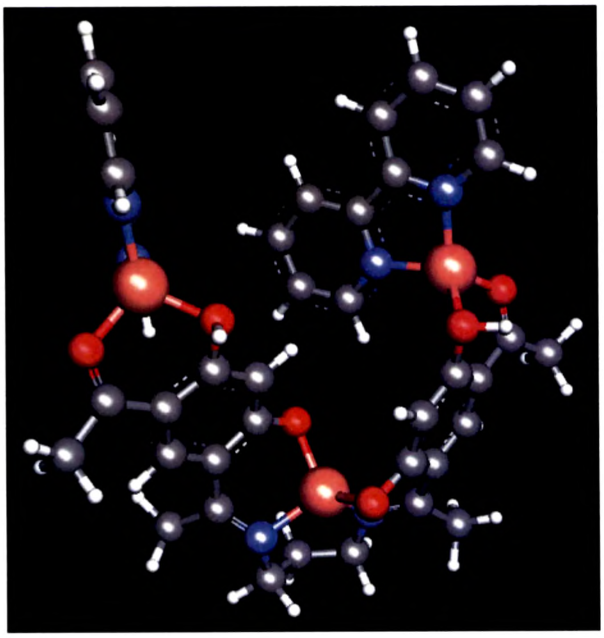

Fig.5.17 Optimized geometry of the complex **[Cu_3dar3pn(bipy)$_2$](ClO_4)$_4$** optimized using UFF.

5.5 ESR Spectra

ESR spectra of two representative complexes **[Cu_3daren(phen)$_2$](ClO_4)$_4$** and **[Cu_3dar2pn(bipy)$_2$](ClO_4)$_4$** were recorded in powder form as well as in solution (DMSO).

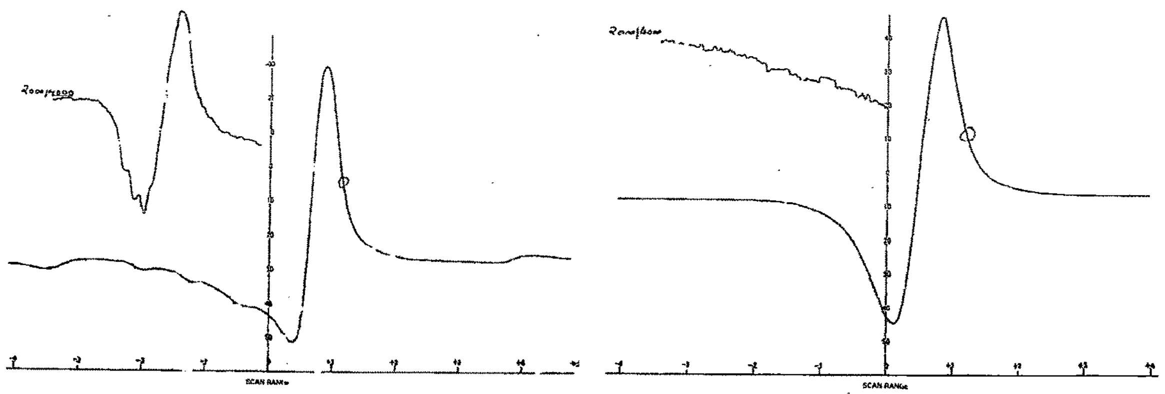

(a) solution **(b) powder**

Fig.5.18 ESR of complex (a) **[Cu_3daren(phen)$_2$](ClO_4)$_4$** and (b) **[Cu_3dar2pn(bipy)$_2$](ClO_4)$_4$**

They are more or less isotropic, with the hyperfine coupling constant A = 160G, indicating the N_2O_2 coordination environment around the copper(II) ions. Complex **[Cu_3daren(phen)$_2$](ClO_4)$_4$** exhibited a well resolved ESR spectrum corresponding to a tricopper(II) system with S = 3/2. Transitions between all the states derived from S =1/2 and S = 3/2 have been observed. These appear at 2352 [(+1/2, 1/2) to (+3/2, 3/2)] and at 3772G [(-1/2, 1/2) to (-3/2, 3/2)]. The presence of the half field transitions in these complexes indicates exchange coupling between the paramagnetic metal centres.

5.6 Magnetic Exchange

The magnetic susceptibility of the complexes **[Cu_3daren(phen)$_2$](ClO_4)$_4$** and **[Cu_3dar2pn(bipy)$_2$](ClO_4)$_4$** was measured from liquid nitrogen (LNT) to room temperature using a Faraday balance. The data was least squares fit to the Van Vleck equation for a linear/angular Cu_3 system using the program Magmum. The representative graphs between the calculated and observed magnetic susceptibility χ_m. and magnetic moment μ verses temperature (K) are shown in **Fig.5.19**. The calculated values of Weiss constant and intramolecular spin coupling constant J are summarized in Table 5.8. As the values suggest there is a weak intermolecular spin coupling in both complexes. The opposite sign of the interaction, however, suggests difference in the packing of the molecules in the solid. The values of coupling constant J_1 between the pair of terminal copper(II) centres varies from weakly antiferromagnetic in the complex **[Cu$_3$daren(phen)$_2$](ClO$_4$)$_4$** to strongly ferromagnetic in **[Cu$_3$dar2pn(bipy)$_2$](ClO$_4$)$_4$**. The values of -J_2 are very high indicating a very strong antiferromagnetic exchange between the neighbouring pairs of copper(II) centres. The geometry of the complexes optimized using universal force field (**Fig.5.20**) shows that the **dar** bridging group is highly planar and has π–delocalisation as discussed earlier. There is an inscribed angle between the copper coordination planes (τ) which depends on the nature of capping bidentate ligand and the aliphatic chain in the trinucleating ligands. The values of J_2 are a function of the dihedral angle τ. As the dihedral angle increases from 122.7 to 130.6 the value of –J_2 increases from 200 to 500cm^{-1}, respectively, in the complexes **[Cu$_3$daren(phen)$_2$](ClO$_4$)$_4$** and **[Cu$_3$dar2pn(bipy)$_2$](ClO$_4$)$_4$**.

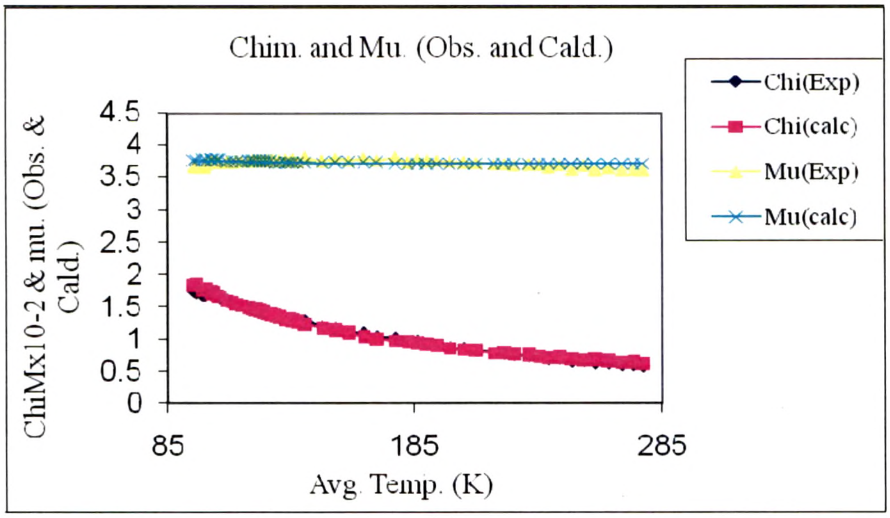

(a)

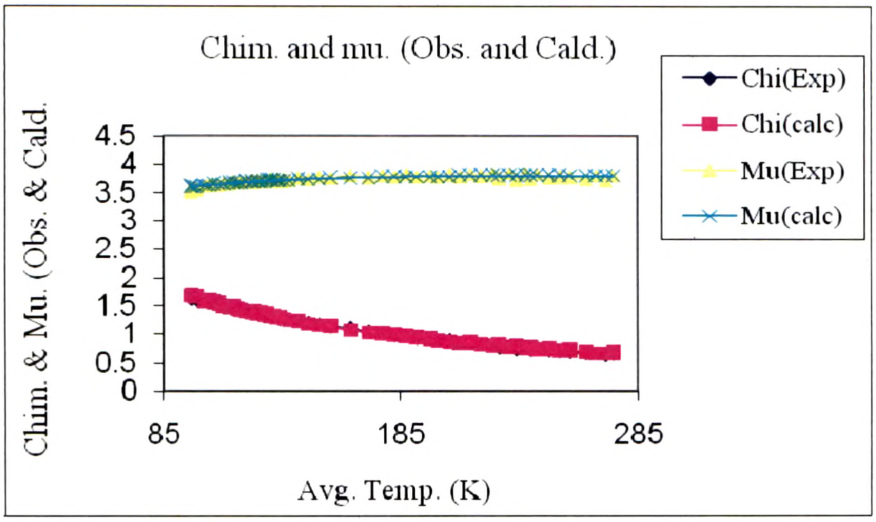

(b)

Fig.5.19 χM v/s T graph for complex, **$[Cu_3daren(phen)_2](ClO_4)_4$ (a),** and **$[Cu_3dar2pn(bipy)_2](ClO_4)_4$ (b).**

Table 5.8 Values of Magnetic exchange parameters.

Complexes	θ	J (cm^{-1})	Dihedral angle
$[Cu_3daren(phen)_2](ClO_4)_4$	15	$J_1 = -16$ $J_2 = -200$	122.68
$[Cu_3dar2pn(bipy)_2](ClO_4)_4$	-10	$J_1 = 337$ $J_2 = -500$	130.62

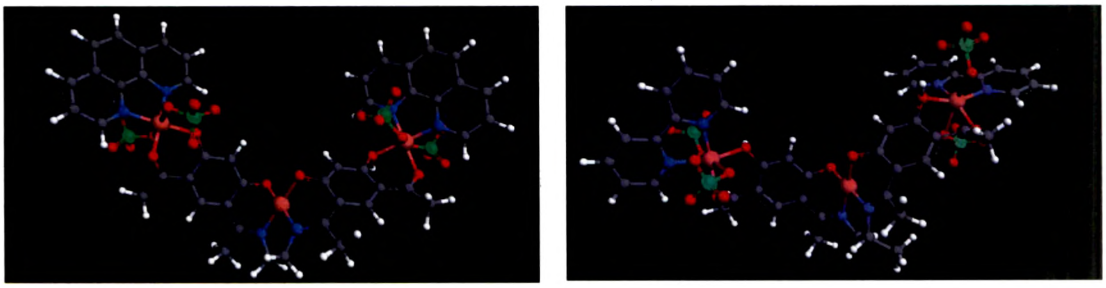

Fig.5.20 Optimized geometries of the complexes **$[Cu_3daren(phen)_2](ClO_4)_4$** and **$[Cu_3dar2pn(bipy)_2](ClO_4)_4$** by UFF method.

5.7 Cyclic Voltametric studies

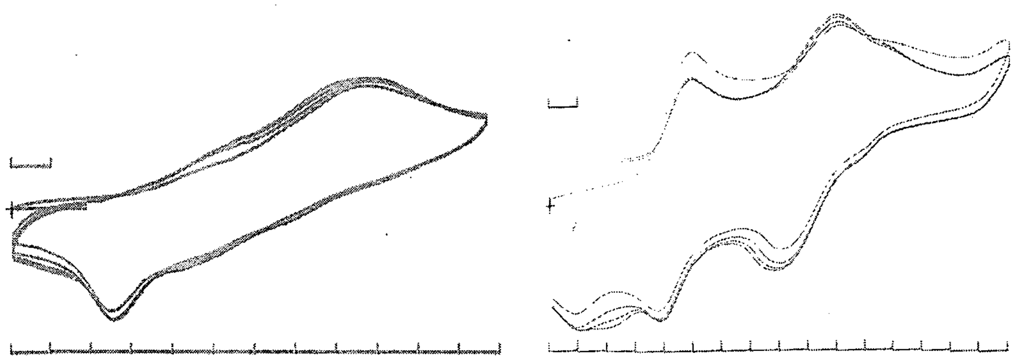

Pt disk working electrode, Pt wire counter electrodes and Ag/AgNO$_3$ (0.1M in CH$_3$CN) as reference electrodes were used.

Fig.5.21 Cyclic voltammogram of complex (a) **[Cu$_3$daren(bipy)$_2$](ClO$_4$)$_4$** and complex (b) **[Cu$_3$dar2pn(bipy)$_2$](ClO$_4$)$_4$**.

The redox potentials observed in the cyclic voltammograms of all the trinuclear complexes are tabulated in (Table 5.9) and typical cyclic voltammograms are shown in (**Fig.5.21**) Redox potentials of complexes are listed below with reference to $C_{p2}Fe/C_{p2}Fe^+$ couple.

Table 5.9 Redox potentials of trinuclear complexes.

Complex	Reduction Potentials			Oxidation Potentials		
	$E_{Pc(1)}$	$E_{Pc(2)}$	$E_{Pc(3)}$	$E_{Pa(1)}$	$E_{Pa(2)}$	$E_{Pa(3)}$
[Cu$_3$daren(phen)$_2$](ClO$_4$)$_4$	-0.517	-0.757	-1.297	-0.157	-0.307	-0.597
[Cu$_3$daren(bipy)$_2$](ClO$_4$)$_4$	-0.532	-0.865	------	-0.282	---	-------
[Cu$_3$dar2pn(phen)$_2$](ClO$_4$)$_4$	-0.515	-0.923	-1.475	-0.263	-0.548	-0.798
[Cu$_3$dar2pn(bipy)$_2$](ClO$_4$)$_4$	-0.523	-1.065	-1.840	-0.407	-0.857	-1.507
[Cu$_3$dar3pn(phen)$_2$](ClO$_4$)$_4$	-0.490	-1.207	-1.257	-0.290	-0.748	-0.757
[Cu$_3$dar3pn(bipy)$_2$](ClO$_4$)$_4$	-0.432	-0.965	-------	-0.298	-0.507	-0.773

The cyclic voltamograms of the complexes recorded between 0.0 to -1.2V potential region indicate, irreversible reductions to copper(I) and copper(0) state in all complexes except **[Cu$_3$daren(bipy)$_2$](ClO$_4$)$_4$**, where the two processes are quasi-reversible. It can be seen from the table that the reduction to copper(I) is variably stepwise or simultaneous. Reduction to copper(0) state appears to be taking place in steps at very close potentials in the complexes, **[Cu_3daren(phen)$_2$](ClO_4)$_4$**, **[Cu_3dar2pn(phen)$_2$](ClO_4)$_4$** and **[Cu_3dar3pn(phen)$_2$](ClO_4)$_4$**. Both of these reduction processes take place at relatively high potential at about -0.8V and approximately -1.2V, respectively. It appears from the voltammograms that, the complexes disintegrate when the reduction of copper to copper(0) state is allowed. This is evident from more than one oxidation processes observed in the second scan at around -0.55V and is reproducible in the subsequent scans. This indicates the formation of relatively stable species in solution after the first cycle.

Noticeably the first reduction process in all the complexes takes place at relatively more negative potentials indicating the presence of strong ligand field and also presence of electron rich ligands confirming the coordination of phenolate. Also it can be seen that at least one of the two reduction processes, $Cu^{II} \rightarrow Cu^{I}$ or $Cu^{I} \rightarrow Cu^{0}$, is simultaneous indicating approximate electronic equivalence of the environment around all the three metal ions.

References:

(1) (a) Li, P.; Solanki, N. K.; Ehrenberg, H.; Feeder, N.; Davis, J. E.; Rawson J. M. and Halcraw, M. A. *J. Chem. Soc. Dalton Trans.,* 2000, 1559. (b) Wrobleski, J. T. and Brown, D. B. *Inorg. Chem.* 1979, **18(10),** 1979. (c) Felthouse, T. R.; Hendrickson, D. N. *Inorg. Chem, 1978, **17**, 444.*

(2) (a) Piperpont, C. G.; Francesconi, L. C.; Hendrickson, D. N. *Inorg. Chem.,* 1978, **17(12),** 3470. (b) Khandagale, P.; Chikate, R.; Joshi, S. B. ; Kulkarni, B. A. *J. of alloys and compounds,* 2005, **392,** 112.

(3) Ward, M. D., *Inorg. Chem.,* **35(6),** 1712.

(4) Niu, S. Y.; Jin, J.; Yong, Z. Z. Synthesis and Reactivity in *Inorganic and Metal-Organic and Nano-Metal chemistry,* 2005, **34,** 173.

(5) Zou, J. Z.; Liu, Q.; Xu, Z.; You, X. Z. and Huang, X. Y. *Polyhedron,* 1998, **17,** 1863.

(6) Kimura, E.; Shionoya, M.; Mita, T.; Itaka, *Y. J. Chem. SOC., Chem. Commun.* 1987, 1712.

(7) Sundberg, R. J. and Martin, R. B. *Chem. Rev.,* 1974, **74,** 471.

(8) Richardson, J. S.; Thomas, K. A.; Rubin, B. H. and Richardson, D. C. *Proc. Natl. Acad. Sci. U. S. A.,* 1975, **72,** 1349.

(9) Fee, J. A. and Briggs, R. G. *Biochim. Biophys. Acta,* 1975, **400,** 439.

(10) Kolks, G.; Fribart, C. R.; Rabinowitz, H. N. and Lippard, S. J.; *J. Am. Chem. Soc.,* 1976, **98,** 5720.

(11) Kolks, G. and Lippard, S. J. *J. Am. Chem.* Soc., 1977, **99,** 5804.

(12) Lundberg, B. K. S. *Acta Chem. Scand.,* 1972, **26,** 3902.

(13) Ivarsson, *G.*; Lundberg, B. K. S. and Ingri, N. *Acta Chem. Scand.,* 1972, 26, 3005.

(14) Goodgame, M. and Cotton, F, A. *J. Am. Chem. Soc.,* 1962, **84,** 1543.

(15) Ghosh, S. P. and Mishra, L. K. *J. Indian Chem.,* 1970, **47,** 1153.

(16) Kaiser, S. W.; Saillant, R. B.; Butler, W. M. and Rasmussen, P. G. *Inorg. Chem.,* 1976, **15,** 2681.

(17) Kaiser, S. W.; Saillant, R. B.; Butler, W. M. and Rasmussen, P. G. *Inorg. Chem.,* 1976, **15,** 2688.

(18) Fieselmann, B. F.; Hendrickson, D. N. and Stucky, G. D. *Inorg. Chem.,* 1978, **17,** 2078.

(19) Brady, J. E. and Fogarty, M. A. C. *J. Inorg. Nucl. Chem.,* 1971, **33,** 2706.

(20) Xu, Z. Ph. D. Thesis, Memorial University of Newfoundland, 1998.

(21) Stratton, W. J. and Busch, D. H. *J. Am. Chem. Soc.,* 1960, **82,** 4834;

(22) Stratton, W. J. And Busch, D. H. *J. Am. Chem. Soc.,* 1958, **80,** 1286;

(23) Stratton, W. J. and Busch, D. H. *J. Am. Chem. Soc.,* 1958, **80,** 3191.

(24) Stratton, W. J.; Ogren, P. *J. Inorg. Chem.,* 1970, **9,** 2588.

(25) Boyd, P. D. W.; Gerloch, M. and Sheldrick, G. M. *J. Chem. Soc., Dalton Trans.,* 1974, 1097.

(26) Saroja, J.; Manivannan, Chakraborty, V.; P. and Pal, S. *Inorg. Chem.,* 1995, **34,** 3099.

(27) O'Connor, C. J.; Romananch, R. J.; Robertson, D. M.; Eduok , E. E. and Fronezek, F. R. *Inorg. Chem.,* 1983, **22,** 449.

(28) Abraham, F.; Lagrence, M.; Sueur, S.; Mernari, B. and Bremard, C. *J. of Chem. Soc., Dalton Trans,* 1991, 1443.

(29) Hasty, E. F.; Colburn, T. J. and Hendrckson, D. N. *Inorg. Chem.*, 1973, **12(10),** 2414.

(30) Decurtins, S.; Schmalle, H. W.; Zheng, L. M. and Ensling, J. *Inorg. Chem. Acta.* 1996, **244,** 165.

(31) Tinti, F.; Verdaguer, M.; Kahn, O.; Savariault, J. M. *Inorg. Chem.,*1994, **26,** 2380.

(32) Li, P.; Solanki, N. K.; Ehrenberg, H. N. Feeder, J.; Davies, E.; Rawson, J. M. and Halcrow, M. A. *J. Chem. Soc., Dalton Trans,* 2000, 1559.

(33) Manada, N.; Okawa, H. and Kida, S. *Bull. of the Chem. Soc. of Jpn.* 1975, **48(1),** 64.

(34) Thomson, L. K.; Mandal, S. K.; Tandon, S. S.; Bridson, J. N. and Park, M. K. *Inorg. Chem.,* **35,** 3117.

(35) Sarakar, S. ; Mondal, A. ; Chopra, D. ; Ribas, J. And Rajak, Kajal, K. *Eur. J. Inorg. Chem.,* 2006, 3510.

(36) Salmon, L.; Thuery, P.; Riviere, E. and Ephritikhine, M. *Inorg. Chem.,* 2006, **45,** 8393.

(37) Graham, B.; Speccia, L.; Fallon, G. D.; Hearn, M. T. W.; Mabbs, F. E.; Moubaraki, B. and Murray, K. S. *J. Chem. Soc., Dalton Trans,* 2001, 1226.

(38) Dong, G.; Chun-qi, Q.; Chun-ying, D.; Ke-liang, P. and Qing-jin, M. *Inorg. Chem.,* 2003, **42,** 2024.

(39) Bian, H.-D.; Gu, W.; Xu, J.-Y.; Bian, F.; Yan, S.-P.; Liao, D.-Z.; Jiang, Z.-H and Cheng, P. *Inorg. Chem.,* 2003, **42,** 4265.

(40) (a) Cotton, F. A.; Lei, B. J.; Lu, T.; Murillo, C. A. *Inorg. Chem.,* 2003, **42,** 3534. (b) Berry, J. F.; Cotton, F. A.; Lu, T.; Murillo, C. A.; Wang, X. *Inorg. Chem.,* 2003, **42,** 3595.

(41) Berry, J. F.; Cotton, F. A.; Lu, T.; Murrilo, C. A. *Inorg. Chem.,* 2003, **42,** 4425.

(42) Thakurta, S.; Chakraborty, J.; Rosair, G.; Tercero, J.; El Fallah, M, S.; Garribba, E. and Mitra, S. *Inorg. Chem.,* 2008, **47,** 6227.

(43) Schmidt, M.W.; Baldridge, K. K.; Boatz, J. A.; Elbert, S. T.; Gordon, M. S.; Jensen, Montgomery, J. A. *J. Comput Chem.* 1993, **14,** 1347.

(44) Ditchfield, R.; Hehre, W. J.; Pople, J. A.; *J. Chem. Phys.* 1971, **54,** 724.

(45) Hehre, W. J.; Ditchfield, R.; Pople, J. A.; *J. Chem. Phys.* 1972, **56,** 2257.

(46) Rassolov, V. A.; Pople, J. A.; Ratner, M. A.; Windus, T. L.; *J. Chem. Phys.* 1998, **109,** 1223.

(47) Casewit, C. J., Colwell, K. S., and Rappe', A. K., *J. Am. Chem. Soc.,* 1992, **114,** 10035.

(48) Casewit, C. J., Colwell, K. S., and Rappe', A. K., *J. Am. Chem. Soc.,*1992, **114,** 10046.

(49) Rappe', A. K. and Goddard, W. A., *J. Phy. Chem.,*1991, **95,** 3358.

(50) Rappe', A. K., Colwell, K. S., and Casewit, C. J., *Inorg. Chem.*1993, **32,** 3438.

(51) Thompson, M. A., Zerner M. C. *J. Am. Chem. Soc.,* 1991, **113,** 8210.

(52) Thompson, Mark A.; Glendening, Eric D. and Feller, David *J. Phys. Chem., 1994,* 10465.

(53) Thompson, Mark A. and Schenter, Gregory K. *J. Phys. Chem.* 1995, **99**, 6374.

(54) Thompson, Mark A.; *J. Phys. Chem.* 1996, **100,** 14492.